International Journal of Numerical Methods for Heat & Fluid Flow

Unsteady MHD boundary layer flow of tangent hyperbolic two-phase nanofluid of moving stretched porous wedge

A. Mahdy, Ali J. Chamkha,

Unsteady MHD boundary layer flow of tangent hyperbolic two-phase nanofluid of moving stretched porous wedge

A. Mahdy
South Valley University, Qena, Egypt, and
Ali J. Chamkha
Department of Mechanical Engineering, Prince Sultan Endowment for Energy and Environment, Prince Mohammad Bin Fahd University, Al-Khobar, Saudi Arabia

Received 6 December 2017
Revised 19 February 2018
Accepted 26 February 2018

Abstract

Purpose – The purpose of this paper is to address the thermo-physical impacts of unsteady magneto-hydrodynamic (MHD) boundary layer flow of non-Newtonian tangent hyperbolic nanofluid past a moving stretching wedge. To delineate the nanofluid, the boundary conditions for normal fluxes of the nanoparticle volume fraction are chosen to be vanish.

Design/methodology/approach – The local similarity transformation is implemented to reformulate the governing PDEs into coupled non-linear ODEs of higher order. Then, numerical solution is obtained for the simplified governing equations with the aid of finite difference technique.

Findings – Numerical calculations point out that pressure gradient parameter leads to improve all skin friction coefficient, rate of heat transfer and absolute value of rate of nanoparticle concentration. As well as, lager values of Weissenberg number tend to upgrade the skin friction coefficient, while power law index and velocity ratio parameter reduce the skin friction coefficient. Again, the horizontal velocity component enhances with upgrading power law index, unsteadiness parameter, velocity ratio parameter and Darcy number and it reduces with rising values of Weissenberg number.

Originality/value – A numerical treatment of unsteady MHD boundary layer flow of tangent hyperbolic nanofluid past a moving stretched wedge is obtained. The problem is original.

Keywords Unsteady, Finite difference, Tangent hyperbolic, Two-phase nanofluid, Wedge

Paper type Research paper

Nomenclature

A = Unsteadiness parameter;
B_0 = Magnetic field;
C_f = Shear stress;
D = Brownian diffusion coefficient;
$\tilde{D}$ = Thermophoresis diffusion coefficient;
Da^{-1} = Darcy number;
F = Non-dimensional stream function;
g = Acceleration due to gravity;
k = Thermal conductivity;
K = Permeability;
Le = Lewis number;

International Journal of Numerical Methods for Heat & Fluid Flow
Vol. 28 No. 11, 2018
pp. 2567-2580

0961-5539
DOI 10.1108/HFF-12-2017-0499

m = pressure gradient parameter;
M_g = Magnetic field parameter;
N_b = Browniam motion parameter;
N_t = Thermophoresis parameter;
Nu = Nusselt number;
Pr = Prandtl number;
Re = Reynolds number;
Sh = Sherwood number;
t = Time;
T = Dimensional temperature;
(u, v) = Velocity components;
U = Ambient velocity;
We = Weissenberg number; and
x, y = Cartesian coordinates.

Greek symbols
σ = Electrical conductivity;
ρ_f = Fluid density (kgm^{-3});
θ = Dimensionless temperature;
ν_f = Kinematic viscosity (m^2s^{-1});
γ^* = Velocity ratio parameter;
ϕ = Dimensionless nanoparticle concentration; and
γ = Time dependent material constant.

Subscripts
w = Conditions at the wall; and
∞ = Conditions in the free stream.

1. Introduction

The researchers either scientists or engineers gave a keen interest to investigate the thermo-physical characteristics of non-Newtonian fluids due to its a variety industrial and technological applications. Pseudo-plasticity represents the main reason of divergence from Newtonian fluid to non-Newtonian fluid, since non-Newtonian fluids have variable viscosity caused by applied force. To analyze non-Newtonian liquids some serious challenges are found, i.e. highly nonlinear of governing boundary layer equations and more complex than Newtonian fluids. As well as, the non-Newtonian fluids diversity leads to no single constitutive equation available to explicate the characteristics of all non-Newtonian fluids. Thus, a number of fundamental equations are suggested to explicate the physical behavior of these fluids. One of the important fluid model in the class of non-Newtonian fluid models is the tangent hyperbolic fluid. This model predicts the phenomenon of shear thinning very accurately as observed from laboratory experiments. Besides, this model explicated the blood flow very precisely. Therefore, some of researchers analyzed the flows of peristaltic with the aid of tangent hyperbolic constitutive equations model. Additionally, the term tangent hyperbolic nanofluid points out the combination of nano-size particles and non-Newtonian tangent hyperbolic fluid. Malik *et al.* (2015) reported the magneto-hydrodynamic (MHD) tangent hyperbolic fluid flow along a stretched cylinder and obtained numerical solution with the aid of Keller-Box method. They depicted that both Weissenberg and Hartmann numbers decline the linear fluid momentum. Akbar (2014) addressed the flow of peristaltic non-Newtonian tangent hyperbolic fluid with convective boundary conditions.

Peristaltic flow of tangent hyperbolic fluid in uniform inclined tube has been discussed by Nadeem and Akbar (2010). Additionally, they obtained series solutions of motion governing equations through homotopy technique and perturbation procedure. Salahuddin *et al.* (2017a, 2017b) performed the aspect of heat generation or absorption on tangent hyperbolic nanofluid nearby the stagnation point along a stretched circular tube. Hayat *et al.* (2016) concerned with the aspects of MHD on peristaltic flow of non-Newtonian hyperbolic tangent nanofluid in an inclined channel in the presence of slip conditions and Joule heating. Mahdy (2014) explored non-Newtonian nanofluid free convection flow relevant to mixed thermal boundary conditions around a vertical cone. Abbas *et al.* (2016) contemplated three dimensional peristaltic of hyperbolic tangent fluid flow in varying channel with flexible surfaces. The flows of boundary layer tangent hyperbolic nanofluid through stretching surfaces with various thermo-physical assumptions have been examined by many of scientists or engineers such as (Hassan *et al.*, 2017; Malik *et al.*, 2016; Bhatti *et al.*, 2017; Sheikholeslami and Chamkha, 2016; Waqas *et al.*, 2016; Akbar *et al.*, 2016; Gorla *et al.*, 2011; Hussain *et al.*, 2017a, 2017b; Chamkha and Rashad, 2014; Khan *et al.*, 2017a, 2017b; Rashad, 2017; Ellahi *et al.*, 2016, Mahdy and Chamkha, 2015; Vargas *et al.*, 1995; Chamkha *et al.*, 2012, 2014, 2015; Ruhaila *et al.*, 2017; Umar *et al.*, 2017).

The MHD flow investigation for an electrically conducting fluid through a heated wedge has significant applications in a number of engineering problems such as MHD power generators, plasma studies, nuclear reactors cooling, petroleum industries, crystal growth and the boundary layer control in aerodynamics. The magnetic nanofluid priority represented in that fluid flow and heat transfer can be controlled by an external source, which yields it applicable to different fields such as thermal engineering, electronic packing and aerospace. Magnetic nanofluid means a magnetic colloidal suspension of both carrier liquid and magnetic nanoparticles. Bilal *et al.* (2017) inspected the flow of MHD Prandtl nanofluid past a stretched sheet and got numerical solution via shooting method. The aspects of viscous dissipation on MHD Sisko fluid flow along a stretched cylinder for the first time has been analyzed by Malik *et al.* (2016). Khan *et al.* (2016) contemplated the MHD non-Newtonian peristaltic movement of non-Newtonian pseudo-plastic fluid flow past asymmetric channel. Numerical solution of stagnation point flow of MHD tangent hyperbolic nanofluid along a stretched cylinder has been obtained by Salahuddin *et al.* (2017a, 2017b). Ellahi *et al.* (2016) exhibited numerical computations of generalized Couette flow of MHD Powell–Eyring fluid with slip condition. Hayat *et al.* (2017) analyzed the aspect of MHD stretched flow of Powell–Eyring fluid past nonlinear stretching surface. Particularly, the MHD flow along a stretching cylinder is considered by Ashorynejad *et al.* (2013). Chamkha *et al.* (2012) exhibited the radiation impact on mixed convection flow past an isothermal vertical wedge immersed in a nanofluid porous medium. Dessie and Kishan (2014) investigated the MHD impacts on regular Newtonian fluid flow over a stretched sheet embedded in a saturated porous media with variable viscosity and heat source/sink. Rahman *et al.* (2012) analyzed the slip of MHD flow and heat generation or absorption aspect on nanofluid boundary layer flow past a wedge. Srinivasacharya *et al.* (2015) concerned with the impact of changeable magnetic field on the fluid flow and heat transfer characteristics past a wedge with variable wall temperature and concentration. Sheikholeslami *et al.* (2016) exhibited the impacts of applied magnetic field on viscous nanofluid flow with the help of Koo-Kleinstreuer (KKL) correlation. Sheikholeslami and Ellahi (2015) chose LBM method to simulate Lorentz force aspect on nanofluid temperature profile. Both of Awais *et al.* (2017) and Hussain *et al.* (2017a, 2017b) exhibited the aspect of normally impinging magnetic field on non-Newtonian Sisko fluid flow along a stretched cylinder with different physical situations.

The main objective of the present perusal is to explicate the MHD unsteady boundary layer flow caused by tangent hyperbolic nanofluid through a moving stretching wedge in a porous medium. Boungiorno model is used to characterize the nanofluid, i.e. the boundary conditions for normal fluxes of the nanoparticle volume fraction are chosen to be zero. A convenient local similar transformations are given to reformulate the governing boundary layer equations into a simple dimensionless form. The finite difference procedure is chosen to get the numerical solution of the resulting system. The aspect of dimensionless parameters on velocity, temperature and nanoparticle volume fraction distributions along with the friction factor, local Nusselt and Sherwood numbers are argued in details with the aid of graphs and tables.

2. Flow model configuration

Let us exhibit the unsteady MHD two-dimensional boundary layer flow of viscous incompressible electrically conducting non-Newtonian tangent hyperbolic nanofluid nearby a non-isothermal stretching wedge moving through porous medium with the velocity $u_w = \frac{ax^m}{1-\lambda t}$. $U(x,t) = \frac{bx^m}{1-\lambda t}$ represents the ambient nanofluid velocity. The nanoparticles volume fraction normal fluxes is chosen to be vanish as the thermophoresis is taken. This leads to the nanoparticles volume fraction at the surface be active control comparing with constant conditions of the nanoparticles volume fraction.

Figure 1 points out that the positive values of x-axis is chosen to be along the wedge surface with the apex as origin. The positive values of y-axis is considered normal to the x-axis in the outward direction towards the fluid. Besides, a transverse magnetic field with uniform strength B_0 is placed perpendicular to the fluid flow direction. Assuming $T_w = T_\infty + \frac{bx^m}{1-\lambda t}$ and T_∞ represent the temperature of the wedge wall and ambient of the nanofluid. Again, C_∞ gives the ambient of fluid nanoparticle volume fraction. The full angle of the wedge is indicated as $\Omega = \beta\pi$, where β gives the gradient of Hartree pressure. It is supposed that both of nanoparticles and base fluid are in thermal equilibrium and the nanoparticles volume fraction normal fluxes is given with zero value as the thermophores is taken in account. Therefore the nanoparticles volume fraction at the surface will be more active control than constant conditions of the nanoparticles volume fraction. The governing PDEs. for the flow of MHD unsteady boundary layer caused by non-Newtonian tangent hyperbolic nanofluid, can be formulated as following:

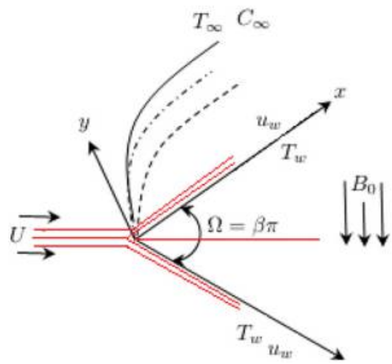

Figure 1.
Coordinate system and physical flow model

$$\frac{\partial u}{\partial x}+\frac{\partial v}{\partial y}=0 \tag{1}$$

$$\begin{aligned}\frac{\partial u}{\partial t}+u\frac{\partial u}{\partial x}+v\frac{\partial u}{\partial y}=\frac{\partial U}{\partial t}+U\frac{\partial U}{\partial x}+\nu_f\left((1-n)+\sqrt{2}n\gamma\frac{\partial u}{\partial y}\right)\frac{\partial^2 u}{\partial y^2}\\ +\left(\frac{\sigma B_0^2}{\rho_f}+\frac{\nu_f}{K}\right)(U-u)\end{aligned} \tag{2}$$

$$\frac{\partial T}{\partial t}+u\frac{\partial T}{\partial x}+v\frac{\partial T}{\partial y}=\alpha_f\frac{\partial^2 T}{\partial y^2}+\left(D\frac{\partial T}{\partial y}\frac{\partial C}{\partial y}+\frac{\tilde{D}}{T_\infty}\left(\frac{\partial T}{\partial y}\right)^2\right) \tag{3}$$

$$\frac{\partial C}{\partial t}+u\frac{\partial C}{\partial x}+v\frac{\partial C}{\partial y}=D\frac{\partial^2 C}{\partial y^2}+\frac{\tilde{D}}{T_\infty}\frac{\partial^2 T}{\partial y^2} \tag{4}$$

the chosen boundary conditions at the wedge surface and far away from it are given as:

$$\begin{cases} u(x,0,t)=u_w(x,t),\ \ v(x,0,t)=0,\ \ T(x,0,t)=T_w(x,t),\ \ \left(D\frac{\partial C}{\partial y}+\frac{\tilde{D}}{T_\infty}\frac{\partial T}{\partial y}\right)_{(x,0,t)}=0 \\ u(x,\infty,t)\to U(x,t),\ \ T(x,\infty,t)\to T_\infty,\ \ C(x,\infty,t)\to C_\infty \end{cases} \tag{5}$$

The nanofluid velocity components in x and y directions are denoted by u, v; respectively; ν_f, α_f, ρ_f, σ and B_0 refer to the base fluid kinematic viscosity, the base fluid thermal diffusivity, the base fluid density, the electrical conductivity and intensity of magnetic field, respectively; D indicates the Brownian diffusion coefficient; $\tilde{D}$ gives the thermophoresis diffusion coefficient; $\tilde{D}$ indicates the heat capacitances ratio; K refers to the permeability; T, C are the temperature and nanoparticle volume fraction; n symbolizes the power law index; γ points out the time dependent material constant; a, b represents positive constants that have dimension reciprocal time. Let us choose the stream function $\psi(x, y)$ which yields the continuity equation 1 that can be satisfied with $u=\frac{\partial\psi}{\partial y}$ and $v=-\frac{\partial\psi}{\partial x}$. To mutate the governing equations into a simple set of ODEs, the following local similarity transformations has been chosen:

$$\eta=\left(\frac{U(1+m)}{2x\nu_f}\right)^{\frac{1}{2}},\ \ \psi=\left(\frac{2x\nu_f U}{1+m}\right)^{\frac{1}{2}}F(\eta),\ \ \theta(\eta)=\frac{T-T_\infty}{T_w-T_\infty},\ \ \ \phi(\eta)=\frac{C-C_\infty}{C_0-C_\infty} \tag{6}$$

Where $C_0=C_\infty+\frac{bx^m}{1-\lambda t}$, by considering the previous local similarity transformations, the PDEs. Equations (2), (3) and (4) are reformulated into dimensionless, non-linear and coupled ODEs as follows:

$$\left((1-n)+nWe\sqrt{1+m}F''\right)\ F'''+FF''+\frac{2m}{1+m}(1-F'^2)+\frac{A}{1+m}(2-2F'-\eta F'')+\frac{2(M_g+Da^{-1})}{1+m}(1-F')=0 \tag{7}$$

$$\frac{1}{Pr}\theta''+N_b\theta'\phi'+N_t\theta'^2+F\theta'-\frac{2m}{1+m}F'\theta-\frac{A}{1+m}(2\theta+\eta\theta')=0 \tag{8}$$

$$\phi''+\frac{N_t}{N_b}\theta''+Pr\,Le\left(F\phi'-\frac{2m}{1+m}F'\phi\right)-\frac{A}{1+m}Pr\,Le(2\phi+\eta\phi')=0 \tag{9}$$

With the following reformulated dimensionless boundary conditions:

$$\begin{cases} F(0)=0,\ \ F'(0)=\gamma^*,\ \ \theta(0)=1,\ \ N_b\phi'(0)+N_t\theta'(0)=0 \\ F'(\infty)\to 1,\ \ \theta(\infty)\to 0,\ \ \phi(\infty)\to 0 \end{cases} \tag{10}$$

With observing that the exponent m (parameter of Falkner–Skan power-law with $0\le m\le 1$) denotes a function of the wedge angle parameter β where the full wedge apex angle is given by $\beta\pi$ such that $m=\frac{\beta}{2-\beta}$. It is clear that $\beta=0$ and $\beta=1$ represents the horizontal and vertical plate cases, respectively. $We=\frac{\gamma U^{3/2}}{\sqrt{\nu_f x}}$ points out the Weissenberg number, $Pr=\frac{\nu_f}{\alpha_f}$, $Le=\frac{\alpha_f}{D}$ refer to the Prandtl and Lewis numbers, $A=\frac{\lambda}{bx^{m-1}}$ means the unsteady parameter, $M_g=\frac{\sigma_f B_0^2 x}{\rho_f U}$ indicates the magnetic field parameter, $N_t=\frac{\tilde{D}(T_w-T_\infty)}{T_\infty \nu_f}$ gives the thermophoresis parameter, $N_b=\frac{D(C_0-C_\infty)}{\nu_f}$ denotes the Brownian motion parameter, $\gamma^*=\frac{b}{a}$ points out the velocity ratio parameter (such that $\gamma^*<0$ gives a stretching wedge, $\gamma^*>0$ gives a contracting wedge and $\gamma^*=0$ gives a fixed wedge, respectively) and $Da^{-1}=\frac{\nu_f x}{KU}$ refers to Darcy number.

Now, both of skin friction coefficient and the local Nusselt and Sherwood numbers are the most significant three physical quantities and are formulated as:

$$C_f=\frac{\tau_w}{\frac{1}{2}\rho_f U^2},\quad Nu=\frac{xq_w}{k_f(T_w-T_\infty)},\quad Sh=\frac{xq_m}{D(C_0-C_\infty)}$$

The three quantities τ_w, q_w and q_m point out the surface shear stress, and the local heat and mass transfer rate per unit area of surface and are given as follows:

$$\tau_w=\mu_f\left((1-n)\frac{\partial u}{\partial y}+\frac{n\gamma}{\sqrt{2}}\left(\frac{\partial u}{\partial y}\right)^2\right)_{y=0},\quad q_w=-k_f\left(\frac{\partial T}{\partial y}\right)_{y=0},\quad q_m=-D\left(\frac{\partial C}{\partial y}\right)_{y=0}$$

In non-dimensional form the skin friction coefficient C_f, the local Nusselt number Nu and the local Sherwood number Sh are formulated as:

$$Re^{\frac{1}{2}}C_f = \left(\sqrt{1+m}(1-n)F''(0) + \frac{1+m}{2}nWeF''(0)^2\right)$$
$$Re^{-\frac{1}{2}}Nu = -\sqrt{1+m}\,\theta'(0), \quad Re^{-\frac{1}{2}}Sh = -\sqrt{1+m}\,\phi'(0) \qquad (11)$$

$Re = \frac{Ux}{2\nu_f L}$ gives the Reynolds number.

3. Solution method

In the introduced flow configuration, the boundary layer flow of unsteady MHD non-Newtonian tangent hyperbolic nanofluid through stretching porous wedge is exhibited. Here, the boundary conditions for normal fluxes of the nanoparticle volume fraction are selected to be vanish. The numerical computations of reformulated equations (equations (7)-(9) concerned with boundary conditions equation (10)) have been calculated with the aid of finite difference technique that called Keller Box which unconditionally stable and possess second order accuracy. This technique was explained by Cebeci and Bradshaw (1984). The step size was selected equals 0.001 and the convergence criteria was chosen to be 10^6. The given asymptotic boundary conditions (equation 10) were exchanged by taking a value of 10 for the similarity variable η_{max} as follows:

$$\eta_{max} = 10, \;\; F'(10) - 1 = \theta(10) = \phi(10) = 0$$

Selecting $\eta_{max} = 10$ leads to all numerical computations approached the asymptotic values accurately. In addition, the thoroughness of computed solution is authenticated by comparing it in specific cases with previous published literature (Khan and Pop, 2013; White, 1991) via Table I. As clear that the introduced numerical method agrees with preceding solutions up to significant number of digits. Now, the graphical results for the problem under consideration from physical view point will be argued.

4. Results and discussion

Numerical computations are brought out for the fluctuations of velocity, temperature and nanoparticle concentration fields across the region of boundary layer to address the aspect of several pertinent physical parameters. These quantities of physical parameters are

m	$F''(0)$ White (1991)	Khan and Pop (2013)	Present
0	0.4696	0.4696	0.46960
$\frac{1}{11}$	0.6550	0.6550	0.65503
$\frac{1}{5}$	0.8021	0.8021	0.80212
$\frac{1}{3}$	0.9276	0.9277	0.92765
$\frac{1}{2}$	1.0389	1.0389	1.03890
1	1.2326	1.2326	1.23258

Table I. Comparison of rate of velocity $F(0)$ for some values of m, as the other parameters are vanish chosen to be vary as following: magnetic field parameter $0 \leq M_g \leq 10$, pressure gradient parameter $0 \leq m \leq 1$, power law index $0 \leq n \leq 0.8$, Weissenberg number $0 \leq We \leq 5$, thermophoresis parameter $0.1 \leq N_t \leq 1$, Brownian motion parameter $0.1 \leq N_b \leq 1$, unsteadiness parameter $0.1 \leq A \leq 5$, Darcy number $0.1 \leq Da^{-1} \leq 10$, Lewis number $0.1 \leq Le \leq 10$ and velocity ratio parameter $0 \leq \gamma^* \leq 1$. Figure 2 delineates the aspects of unsteadiness parameter A on the horizontal component of velocity $F'(\eta)$, temperature $\theta(\eta)$ and nanoparticle concentration $\phi(\eta)$ given by the numerical simulation. The figure interpreted that the velocity field illustrating similar pattern as nanoparticle concentration with unsteadiness parameter, i.e. upgrading behavior of both velocity and nanoparticle concentration for higher values of unsteadiness parameter A. Additionally, the momentum boundary layer is thinner for the larger unsteadiness parameter. Unlike the velocity fields, the temperature of tangent hyperbolic nanofluid curves minimize for higher values of A. Again, the nanoparticle concentration enhances firstly then it reduces. Velocity ratio parameter γ^* influence on the field of horizontal velocity component $F'(\eta)$ is given in the first part of Figure 3. An increment of velocity ratio parameter γ leads to significant aspects on horizontal velocity component field $F'(\eta)$ as given. The velocity curves start from a minimum value at the surface and then upgrade until the maximum value is happened far away from the surface.

The second and third parts of Figure 3 explain the aspect of Weissenberg number We and power law index n on horizontal component of velocity $F'(\eta)$ curves. The two parts of the figure exhibit that the velocity profiles minify with enlarging the Weissenberg number. Physically it holds because Weissenberg number We directly depend on relaxation time, i.e. for larger values of Weissenberg number We relaxation time maximizes and therefore more resistance is induced. Larger values of power law index n leads to an upgrade in velocity curves. Figure 4 explains the fluctuations in the horizontal component of velocity, temperature and nanoparticle concentration profile against magnetic field parameter M_g. Higher values of the magnetic field M_g strongly causes the resistance force contra the fluid movement, which induced an upgrade in the rate of heat transfer inside the boundary layer. It shows that the magnetic field represents one of sources of fluid friction and the heat

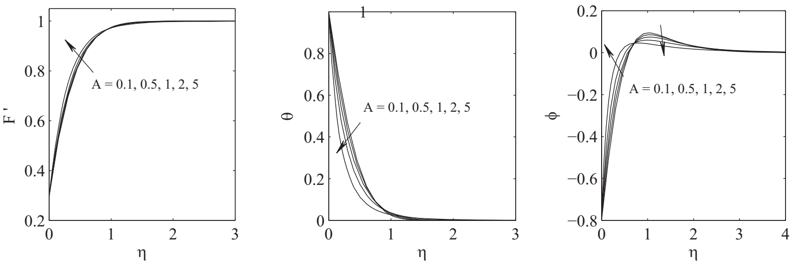

Figure 2.
Impact of A on velocity F', temperature θ and nanoparticle concentration ϕ

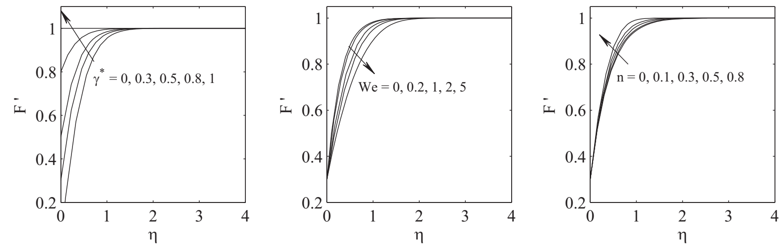

Figure 3.
Impact of velocity ratio parameter γ^*, Weissenberg number We and power law index n on F

transfer. Again, higher values of M_g gives an upgrade of velocity and nanoparticle concentration distribution, whereas the temperature distribution downgrades. In flow of nanofluid, the thermophoresis parameter N_t represents a significant key parameter for analyzing the temperature and nanoparticles concentration distributions. The impact of thermophoresis parameter N_t on the tangent hyperbolic nanofluid temperature and the nanoparticle concentration fields is sketched in first and second parts of Figure 5.

Note, the nanoparticle concentration negative values caused by the fact that the thermophoresis aspect is such that an elevation. Hence, there is found a depression in the nanoparticle concentration relative value at the wall (Kuznetsov and Nield, 2013). The two parts of the figure delineate that higher values of N_t results in upgrading the magnitude of rescaled temperature and the boundary layer thickness of the nanoparticle concentration, therefore improving the absolute value of nanoparticle concentration gradient rate at the surface. This depends on the fact that the force of thermophoresis, which obliges the particles to move from hot to the cold zones, maximizes with rising N_t values. Nanoparticle concentration reduces near to the surface and then an opposite behavior occurs, i.e. it upgrades far away from the surface. Additionally, the Brownian motion parameter N_b can be represented as the ratio of the nanoparticle diffusion (caused by the Brownian motion impact) to the thermal diffusion in the nanofluid. Thus, it is expected that the Brownian motion parameter enlarges with an upgrade in the difference between the nanoparticle concentration at the surface and ambient. Generally, an increment in N_b leads to a downgrade in nanoparticle concentration firstly then it upgrades far away from the surface $\eta \to \infty$, as depicted. A little influence of N_b on nanofluid temperature field is obtained. The aspect of permeability parameter in terms of Darcy number Da^{-1} on the flow velocity field is sketched in First part of Figure 6. Clearly, the flow velocity field and its relevant boundary layer thickness enhance with rising values of Darcy number Da^{-1}. The fluctuations in temperature distribution for some different values of Prandtl number Pr is given in the second part of Figure 6. A major effect on temperature is resulted with an increment in

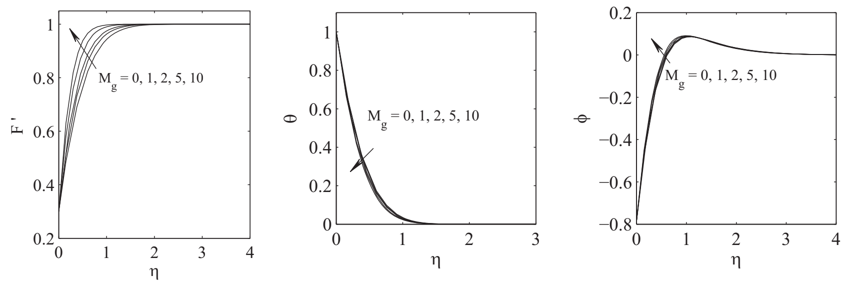

Figure 4. Impact of M_g on Velocity F', temperature θ and nanoparticle concentration ϕ

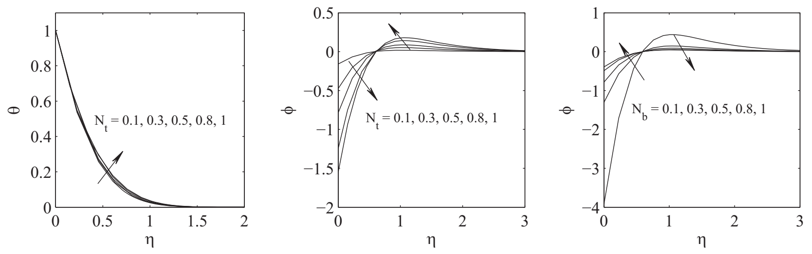

Figure 5. Impact of N_t on temperature θ and nanoparticle concentration ϕ and N_b on ϕ

Prandtl number. The thermal boundary layer thickness minimizes with Prandtl number and it happens due to reduce of thermal diffusivity for enlarging Prandtl number. As thermal conductivity is weakens for higher values of Prandtl number *Pr* which alternatively yields fall down in temperature distribution. Additionally, regular Lewis number *Le* has a significant impact on nanoparticle concentration boundary layer thickness, and it minimizes with larger values of Lewis numbers.

The fluctuations in physical quantities of engineering interest such as skin friction coefficient C_f, Nusselt number *Nu* and Sherwood number *Sh* which describe rate of horizontal velocity component, rate of tangent hyperbolic nanofluid temperature and rate of nanoparticle concentration for some various values of unsteadiness parameter A is delineated in Figure 7. An upgrade is seen in both C_f and *Nu* due to increasing unsteadiness parameter. As clear an increment in unsteadiness parameter A results in reduce the thermal boundary-layer thickness, related to an upgrade in the wall temperature gradient $Re^{-\frac{1}{2}}Nu$, and hence, it yields an enlarge in the surface heat transfer rate. An opposite trend occurs for Sherwood number. The aspect of power law index n, Weissenberg number *We* and velocity ratio parameter γ^* on skin friction coefficient is decelerated in Figure 8. Enlarging both of power law index and velocity ratio parameter yields downgrading in skin friction coefficient, but an opposite behavior is given for Weissenberg number *We*, i.e. the skin friction coefficient upgrades with rising *We*. In view point of physical, as Weissenberg number *We* directly depend on relaxation time, i.e. for higher values of Weissenberg number *We* relaxation time improves and consequently more resistance is generated.

The variations in skin friction coefficient C_f, Nusselt number *Nu* and Sherwood number *Sh* versus some various values of pressure gradient parameter m is displayed in Figure 9. An upgrade is obtained in both C_f and *Nu* caused by increasing pressure gradient parameter m, whereas an opposite behavior occurs of Sherwood number. The effect of thermophoresis parameter N_t on Nusselt number and Sherwood number is illustrated in first and second parts of Figure 10. Clearly, rising N_t leads to reduce rate of both heat transfer and

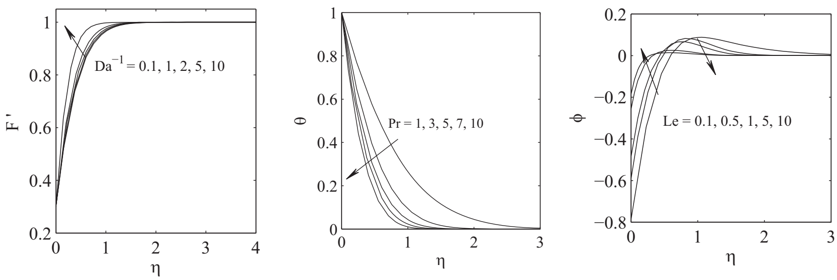

Figure 6.
Impact of D^{-1} on Velocity F', Pr on temperature θ and Le on nanoparticle concentration ϕ

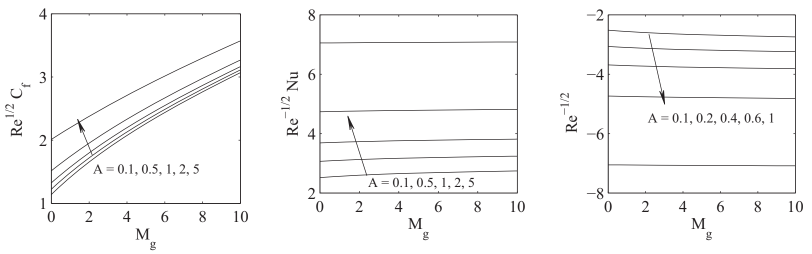

Figure 7.
Impact of unsteadiness parameter A on $Re^{\frac{1}{2}}C_f$, $Re^{-\frac{1}{2}}Nu$ and $Re^{-\frac{1}{2}}Sh$

nanoprticle concentration which is given in terms of Nusselt number Nu and Sherwood number Sh. As the third part of Figure 10 shows the rate of nanoparticle concentration upgrades with enlarging Brownian motion parameter N_b.

5. Remarks

Presented analysis delineates the numerical solution of unsteady non-Newtonian tangent hyperbolic nanofluid flow past a stretching porous wedge with the aspect of magnetic field. Chosen model for tangent hyperbolic nanofluid involves the aspects of both thermophoresis and Brownian motion. With the aid of an implicit finite difference technique, a similar solution of reformulated boundary value problem has been gotten which depends on Darcy number Da^{-1}, unsteady parameter A, Hartmann number M_g, power law index n, Lewis number Le, Weissenberg number We, Prandtl number Pr, velocity ratio parameter γ^*, Brownian motion parameter N_b, pressure gradient parameter m and thermophoresis number N_t. The main outcomes of the present flow are cataloged as follows:

- The horizontal velocity component enhances with upgrading power law index n, unsteadiness parameter A, velocity ratio parameter γ^* and Darcy number Da^{-1}. It reduces with rising values of Weissenberg number We.

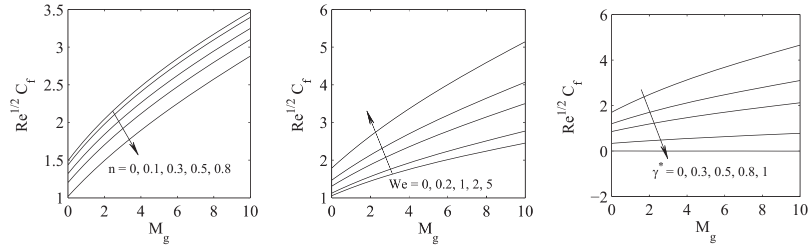

Figure 8. Impact of power law index n, Weissenberg number We and velocity ratio parameter γ^* on $Re^{\frac{1}{2}}C_f$

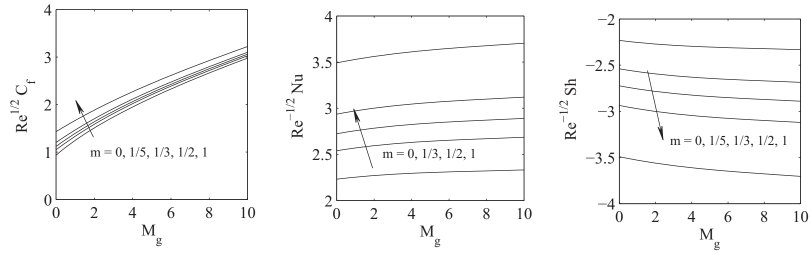

Figure 9. Impact of pressure gradient parameter m on $Re^{\frac{1}{2}}C_f$, $Re^{-\frac{1}{2}}Nu$ and $Re^{-\frac{1}{2}}Sh$

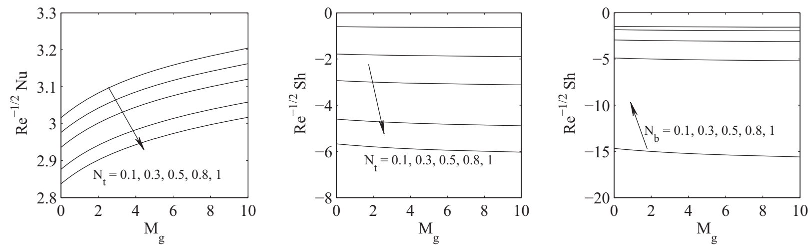

Figure 10. Impact of thermophoresis parameter N_t on $Re^{-\frac{1}{2}}Nu$, $Re^{-\frac{1}{2}}Sh$ and N_b on $Re^{-\frac{1}{2}}Sh$

- Rising values of thermophoresis parameter tends to improve both the temperature and nanoparticle concentration distributions. The Brownian motion parameter has negative aspect on the nanoparticle concentration field.
- Pressure gradient parameter m leads to improve all skin friction coefficient, rate of heat transfer and absolute value of rate of nanoparticle concentration.
- Larger values of Weissenberg number We tends to boost the skin friction coefficient, while n and γ^* reduce the skin friction coefficient.

References

Abbas, M.A., Bai, Y.Q., Bhatti, M.M. and Rashidi, M.M. (2016), “Three dimensional peristaltic flow of hyperbolic tangent fluid in non-uniform channel having flexible walls”, *Alexandria Engineering Journal*, Vol. 55 No. 1, pp. 653-662.

Akbar, N.S. (2014), “Peristaltic flow of a tangent hyperbolic fluid with convective boundary condition”, *The European Physical Journal Plus*, Vol. 129 No. 10, pp. 1-10.

Akbar, N.S., Raza, M. and Ellahi, R. (2016), “Copper oxide nanoparticles analysis with water as base fluid for peristaltic flow in permeable tube with heat transfer”, *Computer Methods and Programs in Biomedicine*, Vol. 130, pp. 22-30.

Ashorynejad, H.R., Sheikholeslami, M., Pop, I. and Ganji, D.D. (2013), “Nanofluid flow and heat transfer due to a stretching cylinder in the presence of magnetic field”, *Heat and Mass Transfer*, Vol. 49 No. 3, pp. 427-436.

Awais, M., Malik, M.Y., Bilal, S., Salahuddin, T. and Hussain, A. (2017), “Magnetohydrodynamic (MHD) flow of sisko fluid near the axisymmetric stagnation point towards a stretching cylinder”, *Results in Physics*, Vol. 7, pp. 49-56.

Bhatti, M.M., Zeeshan, A., Ellahi, R. and Ijaz, N. (2017), “Heat and mass transfer of two-phase flow with electric double layer effects induced due to peristaltic propulsion in the presence of transverse magnetic field”, *Journal of Molecular Liquids*, Vol. 230, pp. 237-246.

Bilal, S., Rehman, K.U., Malik, M.Y., Hussain, A. and Awais, M. (2017), “Effect logs of double diffusion on mhd prandtl nano fluid adjacent to stretching surface by way of numerical approach”, *Results in Physics*, Vol. 7, pp. 470-479.

Cebeci, T. and Bradshaw, P. (1984), *Physical and Computational Aspects of Convective Heat Transfer*, Springer-Verlag, NewYork.

Chamkha, A.J. and Rashad, A.M. (2014), “MHD forced convection flow of a nanofluid adjacent to a non-isothermal wedge”, *Computational Thermal Sciences*, Vol. 6 No. 1, pp. 27-39.

Chamkha, A.J., Abbasbandy, S. and Rashad, A.M. (2015), “Non-Darcy natural convection flow of non-newtonian nanofluid over a cone saturated in a porous medium with uniform heat and volume fraction fluxes”, *International Journal of Numerical Methods for Heat and Fluid Flow*, Vol. 25 No. 2, pp. 422-437.

Chamkha, A.J., Rashad, A.M. and Gorla, R. (2014), “Non-Similar solutions for mixed convection along a wedge embedded in a porous medium saturated by a non-Newtonian nanofluid”, *International Journal of Numerical Methods for Heat and Fluid Flow*, Vol. 24 No. 7, pp. 1471-1486.

Chamkha, A.J., Abbasbandy, S., Rashad, A.M. and Vajravelu, K. (2012), “Radiation effects on mixed convection over a wedge embedded in a porous medium filled with a nanofluid”, *Transport in Porous Media*, Vol. 91 No. 1, pp. 261-279.

Dessie, H. and Kishan, N. (2014), “MHD effects on heat transfer over stretching sheet embedded in porous medium with variable viscosity, viscous dissipation and heat source/sink”, *Ain Shams Engineering Journal*, Vol. 5 No. 3, pp. 967-077.

Ellahi, R., Hassan, M. and Zeeshan, A. (2016), "Aggregation effects on water base Al2O3nanofluid over permeable wedge in mixed convection", *Asia-Pacific Journal of Chemical Engineering*, Vol. 11 No. 2, pp. 179-186.

Ellahi, R., Shivanian, E., Abbasbandy, S. and Hayat, T. (2016), "Numerical study of magneto-hydrodynamics generalized couette flow of Eyring–Powell fluid with heat transfer and slip condition", *International Journal of Numerical Methods for Heat and Fluid Flow*, Vol. 26 No. 5, pp. 1433-1445.

Gorla, S.R.R., Chamkha, A.J. and Rashad, A.M. (2011), "Mixed convective boundary layer flow over a vertical wedge embedded in a porous medium saturated with a nanofluid: natural convection dominated regime", *Nanoscale Research Letters*, Vol. 6 No. 1, pp. 207-216.

Hassan, M., Zeeshan, A., Majeed, A. and Ellahi, R. (2017), "Particle shape effects on ferrofluids flow and heat transfer under influence of low oscillating magnetic field", *Journal of Magnetism and Magnetic Materials*, Vol. 443, pp. 36-44.

Hayat, T., Shafique, M., Tanveer, A. and Alsaedi, A. (2016), "Magnetohydrodynamic effects on peristaltic flow of hyperbolic tangent nanofluid with slip conditions and joule heating in an inclined channel", *International Journal of Heat and Mass Transfer*, Vol. 102, pp. 54-63.

Hayat, T., Sajjad, R., Muhammad, T., Alsaedi, A. and Ellahi, R. (2017), "On MHD nonlinear stretching flow of Powell–Eyring nanomaterial", *Results in Physics*, Vol. 7, pp. 535-5343.

Hussain, A., Malik, M.Y., Bilal, S., Awais, M. and Salahuddin, T. (2017a), "Computational analysis of magnetohydrodynamic sisko fluid flow over a stretching cylinder in the presence of viscous dissipation and temperature dependent thermal conductivity", *Results in Physics*, Vol. 7, pp. 139-146.

Hussain, A., Malik, M.Y., Salahuddin, T., Bilal, S. and Awais, M. (2017b), "Combined effects of viscous dissipation and joule heating on MHD sisko nanofluid flow over stretching cylinder", *Journal of Molecular Liquids*, Vol. 231, pp. 341-345.

Khan, W.A. and Pop, I. (2013), "Boundary layer flow past a wedge moving in a nanofluid", *Mathematical Problems in Engineering*, Vol. 53 Nos. 11/12, pp. 2477-2483.

Khan, A.A., Muhammad, S., Ellahi, R. and Zaigham Zia, Q.M. (2016), "Bionic study of variable viscosity on MHD peristaltic flow of pseudoplastic fluid in an asymmetric channel", *Journal of Magnetism and Magnetic Materials*, Vol. 21 No. 2, pp. 273-280.

Khan, M., Malik, M.Y., Salahuddin, T. and Khan, I. (2017a), "Numerical modeling of carreau fluid due to variable thicked surface", *Results in Physics*, Vol. 7, pp. 2384-2390.

Khan, U., Ahmed, N., Bin-Mohsen, B. and Mohyud-Din, S.T. (2017b), "Nonlinear radiation effects on flow of nanofluid over a porous wedge in the presence of magnetic field", *International Journal of Numerical Methods for Heat and Fluid Flow*, Vol. 27 No. 1, pp. 48-63.

Kuznetsov, A.V. and Nield, D.A. (2013), "The Cheng-Minkowycz problem for natural convective boundary layer flow in a porous medium saturated by a nanofluid: a revised model", *International Journal of Heat and Mass Transfer*, Vol. 65, pp. 682-685.

Mahdy, A. (2014), "Non-Newtonian nanofluid free convection flow subject to mixed thermal boundary conditions about a vertical cone 2014", *Journal of the Brazilian Society of Mechanical Sciences and Engineering*, Vol. 36 No. 4, pp. 951-960.

Mahdy, A. and Chamkha, A.J. (2015), "Heat transfer and fluid flow of a non-Newtonian nanofluid over an unsteady contracting cylinder employing buongiorno's model", *International Journal of Numerical Methods for Heat and Fluid Flow*, Vol. 25 No. 4, pp. 703-723.

Malik, M.Y., Hussain, A., Salahuddin, T. and Awais, M. (2016), "Effects of viscous dissipation on MHD boundary layer flow of sisko fluid over a stretching cylinder", *AIP Advances*, Vol. 6 No. 3, p. 035009.

Malik, M.Y., Hussain, A., Salahuddin, T., Awais, M., Bilal, S. and Khan, F. (2016), "Flow of sisko fluid over a stretching cylinder and heat transfer with viscous dissipation and variable thermal conductivity: a numerical study", *AIP Advances*, Vol. 6 No. 2, p. 045118.

Malik, M.Y., Salahuddin, T., Hussain, A. and Bilal, S. (2015), "MHD flow of tangent hyperbolic fluid over a stretching cylinder using Keller-Box method", *Journal of Magnetism and Magnetic Materials*, Vol. 395, pp. 271-276.

Nadeem, S. and Akbar, N.S. (2010), "Series solutions for the peristaltic flow of a tangent hyperbolic fluid in a uniform inclined tube", *Zeitschrift Für Naturforschung A*, Vol. 65 No. 11, pp. 887-895.

Rahman, M.M., Al-Lawatia, M.A., Eltayeb, I.A. and Al-Salti, N. (2012), "Hydromagnetic slip flow of water based nanofluids past a wedge with convective surface in the presence of heat generation (or) absorption", *International Journal of Thermal Sciences*, Vol. 57, pp. 172-182.

Rashad, A.M. (2017), "Impact Of thermal radiation on MHD slip flow of a ferrofluid over a nonisothermal wedge", *Journal of Magnetism and Magnetic Materials*, Vol. 422, pp. 25-31.

Salahuddin, T., Khan, I., Malik, M.Y., Khan, M., Hussain, A. and Awais, M. (2017a), "Internal friction between fluid particles of MHD tangent hyperbolic fluid with heat generation: using coefficients improved by cash and karp", *The European Physical Journal Plus*, Vol. 132 No. 5, pp. 205-214.

Salahuddin, T., Malik, M.Y., Hussain, A., Awais, M., Khan, I. and Khan, M. (2017b), "Analysis of tangent hyperbolic nanofluid impinging on a stretching cylinder near the stagnation point", *Results in Physics*, Vol. 7, pp. 426-434.

Sheikholeslami, M. and Chamkha, A.J. (2016), "Flow and convective heat transfer of a ferro-nanofluid in a double-sided lid-driven cavity with a wavy wall in the presence of a variable magnetic field", *Numerical Heat Transfer, Part A: Applications*, Vol. 69 No. 10, pp. 1186-1200.

Sheikholeslami, M. and Ellahi, R. (2015), "Three dimensional mesoscopic simulation of mag-netic field effect on natural convection of nanofluid", *International Journal of Heat and Mass Transfer*, Vol. 89, pp. 799-808.

Sheikholeslami, M., Zaigham Zia, Q.M. and Ellahi, R. (2016), "Influence of induced magnetic field on free convection of nanofluid considering Koo-Kleinstreuer (KKL) correlation", *Applied Sciences*, Vol. 6 No. 11, p. 324.

Srinivasacharya, D., Upendar, M. and Venumadhav, K. (2015), "MHD boundary layer flow of a nanofluid past a wedge", *Procedia Engineering*, Vol. 127, pp. 1064-1070.

Vargas, J.V.C., Laursen, T.A. and Bejan, A. (1995), "Nonsimilar solutions for mixed convection on a wedge embedded in a porous medium", *International Journal of Heat and Fluid Flow*, Vol. 16 No. 3, pp. 211-216.

Waqas, M., Hayat, T., Farooq, M., Shehzad, S.A. and Alsaedi, A. (2016), "Cattaneo-Christov heat flux model for flow of variable thermal conductivity generalized burgers fluid", *Journal of Molecular Liquids*, Vol. 220, pp. 642-648.

White, F.M. (1991), *Viscous Fluid Flow*, 2nd, ed. McGraw-Hill, New York, NY.

Further reading

Kasmani, R.M., Sivasankaran, S., Bhuvaneswari, M. and Hussein, A.K. (2017), "Analytical and numerical study on convection of nanofluid past a moving wedge with soret and dufour effects", *International Journal of Numerical Methods for Heat and Fluid Flow*, Vol. 27 No. 10, pp. 2333-2354.

Corresponding author

Ali J. Chamkha can be contacted at: achamkha@pmu.edu.sa